Formation, possible detection and consequences of highly magnetized compact stars

Banibrata Mukhopadhyay

Indian Institute of Science (IISc) Bangalore

Collaborators (inter-continental): Srishty Aggarwal (IISc), Mukul Bhattacharya (Virginia-Tech/Penn-State), Tomasz Bulik (Warsaw), Upasana Das (Cactus Comm.), Debabrata Deb (IISc), Abhay Gupta (New South Wales), Gianluca Gregori (Oxford), Alexander Hackett (Cambridge), Surajit Kalita (IISc), Drisya Karinkuzhi (IISc), Tushar Mondal (IISc), Arnab Sarkar (IISERK/Cambridge), Armen Sedrakian (Frankfurt), Monika Sinha (IITJ), Christopher Tout (Cambridge), Fridolin Weber (SDSU/UCSD)

The Modern Physics of Compact Stars and Relativistic Gravity 2021
September 27-30, 2021, Yerevan, Armenia (Presented Virtually)

Highlights

- ❑ Over last several years, there are lots of interest in massive compact objects, with their several direct/indirect evidences

- ❑ GW190814 confirms existence of a compact star of mass 2.5-2.67 solar mass → in so-called mass gap → massive neutron stars?

- ❑ Since last 15 years or so, at least a dozen evidences for SNeIa are, whose peculiarity lies with lightcurve, its over-luminosity and low ejecta velocity

- ❑ Arguing super-Chandrasekhar progenitor white dwarf

- ❑ Approach: compact objects (1) with strong magnetic field, (2) in modified gravity, (2) matter encountering noncommutative physics at high density, (3) having Ungravity effect, (4) having net charge, (5) having many variant magnetic fields, anisotropic matter and field effects (*see the next talk*)

- ❑ Since last one decade or so, we have been enlightening issue by magnetic field and modified gravity

- ❑ Other consequences: white dwarf pulsars, gravitational radiation, SGRs/AXPs, etc.

- ❑ Brings super-Chandrasekhar white dwarfs in lime-light → many groups joined working in the field → not necessarily high magnetic field based idea

- ❑ Leading to their mass-radius relation, e.g. for white dwarf, different than that of Chandrasekhar → could be prolate/oblate spheroid

All SNeIa data

Taubenberger 2017

Handbook of Supernovae', edited by A. Alsabti and P. Murdin, Springer.

Present talk primarily focuses on magnetized white dwarfs

↓

Following talk by Debabrata Deb will take over neutron/strange stars

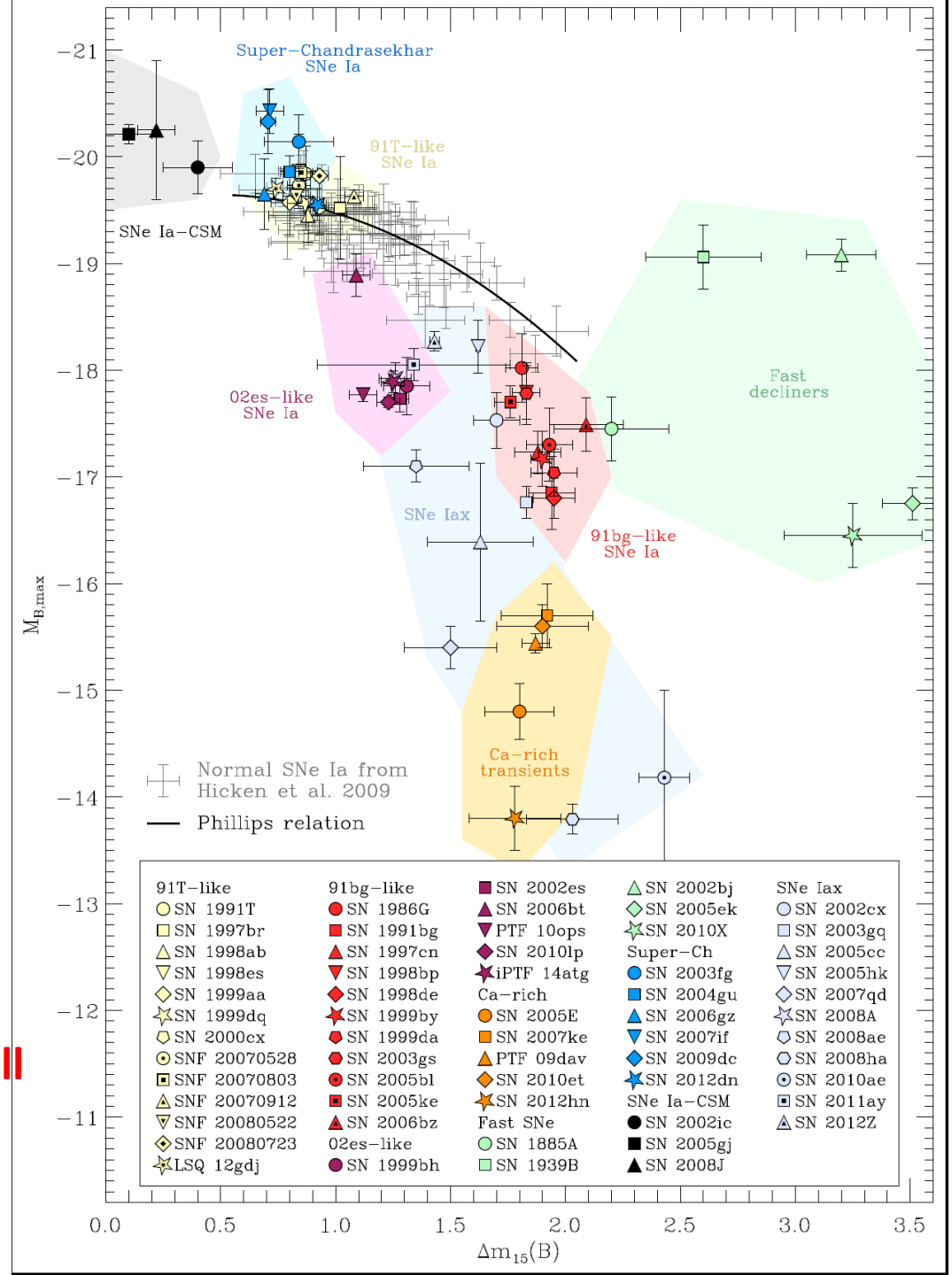

How strong field could be in dynamo and geometry?

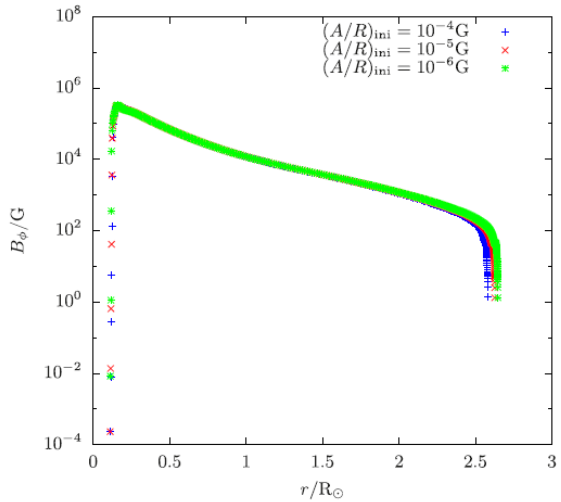

Figure 7. Toroidal field in the interior of the star as a function of the radius at the end of the main sequence.

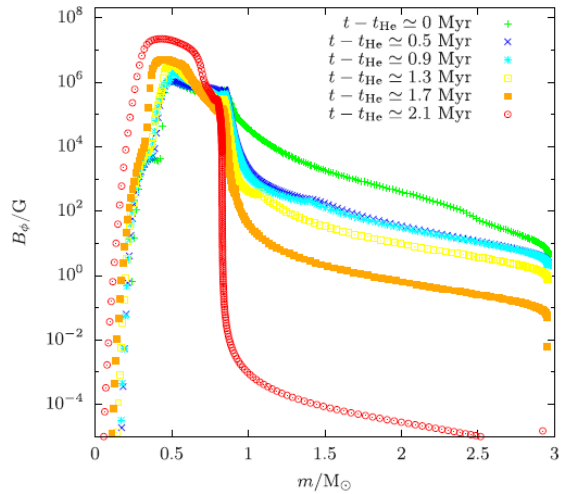

Figure 15. Toroidal field inside the star as a function of the mass coordinate at various times after helium exhaustion in the core, at time $t_{\rm He}$, during the asymptotic giant phase.

- Dynamo based simulations by STARS argue that at end of main sequence, star will have toroidally dominated magnetic fields

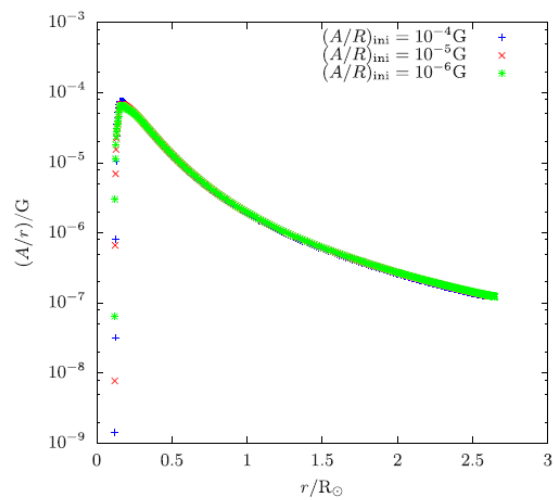

Figure 8. Poloidal field in the interior of the star as a function of the radius at the end of the main sequence.

- Field decays from center to surface

- For magnetic field ~ 10^8 G for star of size 10^6 km
- Flux ~ 10^{20} G km^2
- For a 1000km size white dwarf, B ~ 10^{14} G

Wickramasinghe, Tout & Ferrario, MNRAS 2014; Quentin & Tout, MNRAS 2018; BM, Sarkar & Tout, MNRAS 2020; Bhattacharya et al., MNRAS (submitted)

Virial theorem based argument

$$-\alpha\frac{GM^2}{R}+\beta\frac{M^\Gamma}{R^{3(\Gamma-1)}}+\gamma\frac{\Phi_M^2}{R}=0,$$

Gravity Thermal Magnetic

$$\alpha=\frac{3(\Gamma_1-1)}{5\Gamma_1-6},$$

$$\beta=\left(1+\frac{\Gamma-\Gamma_1}{(5\Gamma_1-6)(\Gamma-1)}\right)\frac{3^\Gamma K}{(4\pi)^{\Gamma-1}},$$

$$\gamma=\frac{1}{6}.$$

$$M=\sqrt{\frac{\gamma\Phi_M^2}{\alpha G\left(1-\frac{\beta M^{\Gamma-2}}{\alpha G R^{3\Gamma-4}}\right)}}$$

$$\frac{1}{\rho}\left(\frac{\mathrm{d}P}{\mathrm{d}r}+\frac{\mathrm{d}P_B}{\mathrm{d}r}\right)=-\frac{Gm(r)}{r^2}$$

$$P=K\rho^\Gamma \quad P_B=K_1\rho^{\Gamma_1}$$

With, e.g., $\Gamma=4/3$, $\Gamma_1=1.8$
$\alpha\downarrow$, $\beta\downarrow$, β/α fixed

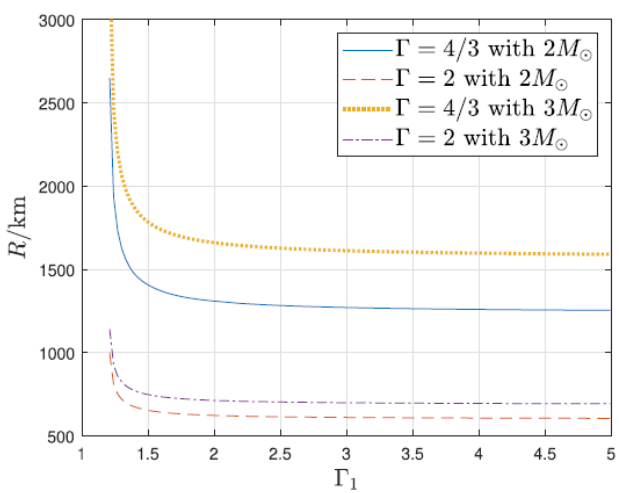

Figure 8. Variation of the radius R with Γ_1 for the *Power Law* model with various Γ and total masses. In each case, $\Gamma=4/3$ corresponds to $\overline{B}=10^{14}$ G and $\Gamma=2$ corresponds to $\overline{B}=10^{16}$ G.

Equilibrium solution of mass 2-3$M_\odot$ is possible depending on EoS (i.e. Γ or field)

This gives us more confidence to explore full-scale numerical calculation of stellar structure with strong field and finite temperature

BM, Sarkar, Tout, MNRAS 2021

Fossil origin of strong field

Growth: mass of the white dwarf Increases due to accretion → gravitational power increases over degeneracy pressure → star contracts → any initial seed magnetic field (B) increases as "B π r^2 " is conserved

Magnetostatic equilibrium: once B increases, total outward force further increases balancing gravitational force → Repetition of above cycle

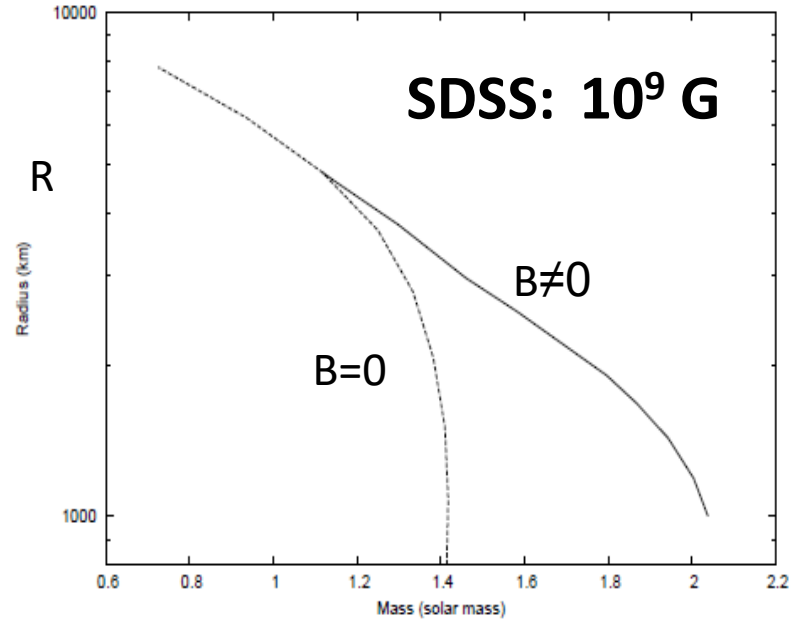

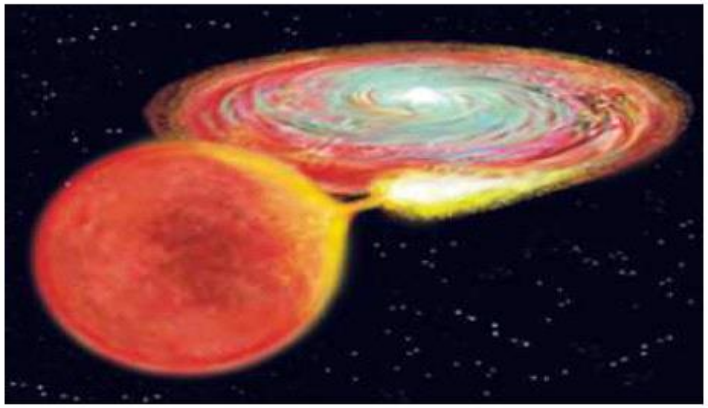

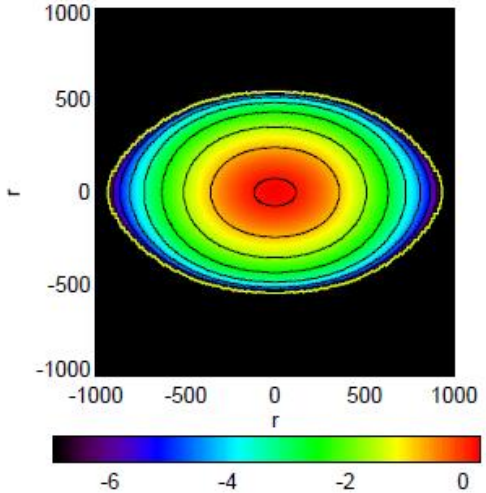

Subramanian, BM, MNRAS 2015

Das, BM, Rao, ApJL 2013

Evolution of white dwarfs

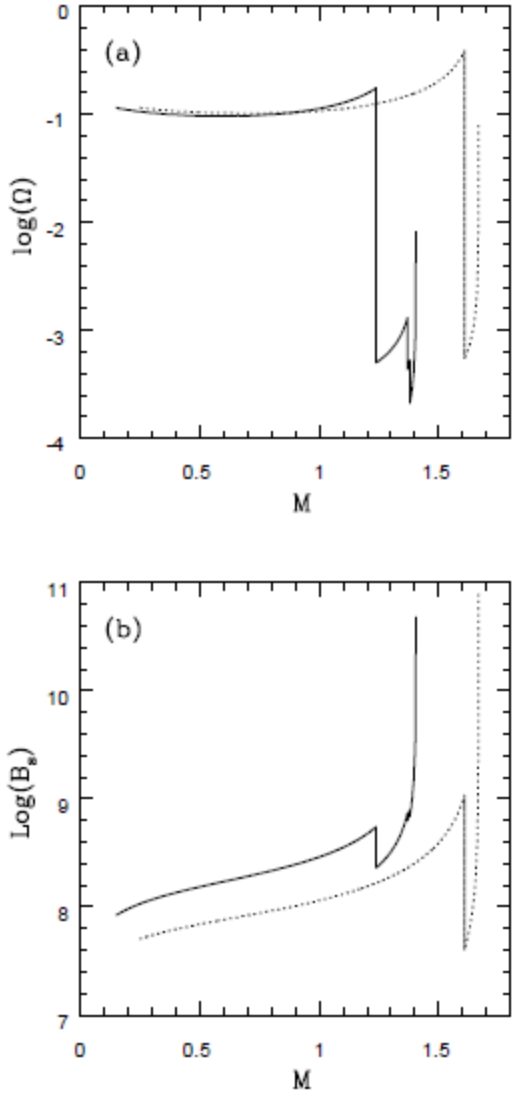

Figure 2. Time evolution of (a) angular velocity in sec^{-1}, (b) magnetic field in G, as functions of mass in units of solar mass. The solid curves correspond to the case with $n = 3$, $m = 2.7$, $\rho = 0.05$ gm cm^{-3}, $l = 1.5$ and dotted curves correspond to the case with $n = 3$, $m = 2$, $\rho = 0.1$ gm cm^{-3}, $l = 2.5$. Other parameters are $k = 10^{-14}$ CGS, $\dot{M} = 10^{-8} M_{\odot} \mathrm{Yr}^{-1}$, $\alpha = 10$ degree and $R = 10^4$ km at $t = 0$.

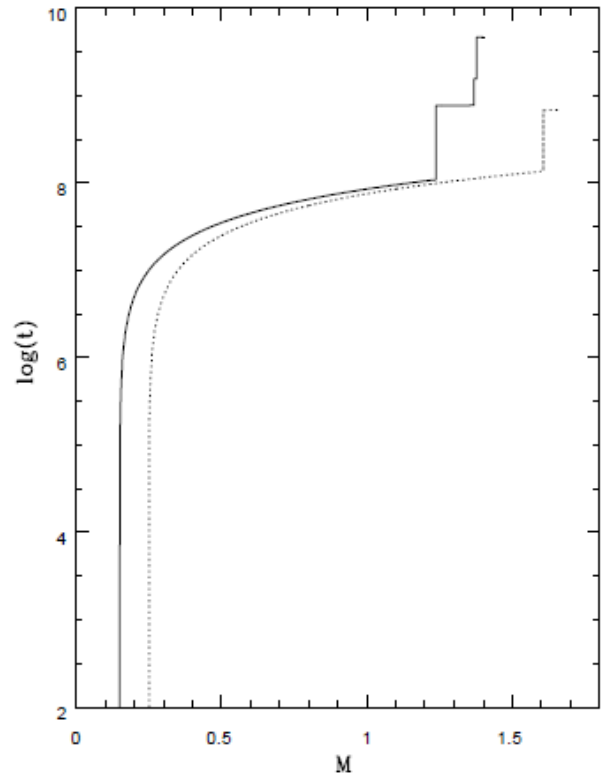

BM, Rao, Bhatia, MNRAS 2017

Neglecting detailed CV physics

Figure 4. Time taken in Yr to evolve the mass and magnetic fields of white dwarfs shown in Fig. 2.

$$\dot{\Omega} = k\Omega^n$$

Accretion phase

$$l\Omega(t)^2 R(t) = \frac{GM(t)}{R(t)^2},$$

$$I(t)\Omega(t) = \text{constant},$$

$$B_s(t)R(t)^2 = \text{constant},$$

Spin-powered phase

$$\Omega = \left[\Omega_0^{1-n} - k(1-n)(t-t_0)\right]^{\frac{1}{1-n}},$$

$$B_s = \sqrt{\frac{5c^3 I k \Omega^{n-m}}{R^6 \sin^2\alpha}},$$

$$-\frac{GM}{R^2} = \frac{1}{\rho}\frac{d}{dr}\left(\frac{B^2}{8\pi}\right)|_{r=R} \sim -\frac{B_s^2}{8\pi R\rho},$$

n=m=3: dipole

Rotating Magnetized White Dwarfs

ME/GE, KE/GE are in accordance with Braithwaite 2009; Komatsu et al. 1989

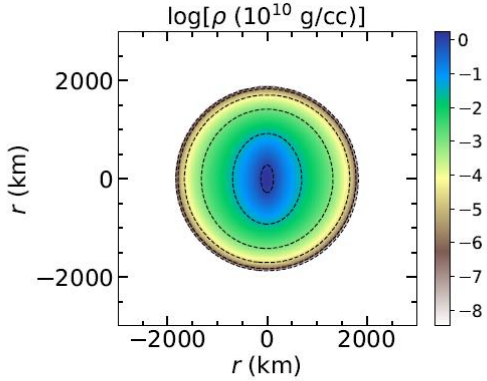

(a) Ω = 0.0628 rad/s

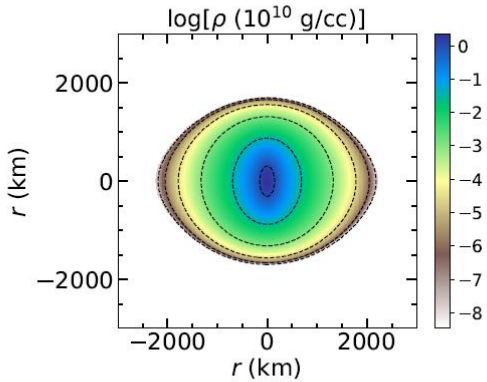

(b) Ω = 3.6537 rad/s

Figure 2. Density isocontours of uniformly rotating white dwarf with toroidal magnetic field.

Uniform rotation:
Mass varying from
1.4-1.8 $M_\odot$ for
0.004< ME/GE < 0.12
←

Ω_c = 30 rad/s

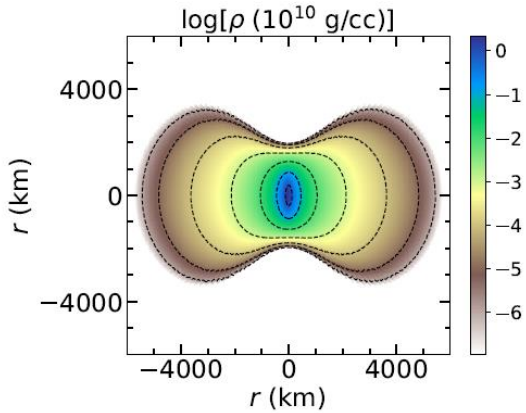

(a) Toroidal magnetic field

Density contours for purely toroidal field configuration with different angular velocity and A^2 ~ 10^5

$$A^2(\Omega_c - \Omega) = \frac{(\Omega - \omega) r^2 \sin^2\theta e^{2(\beta-\nu)}}{1-(\Omega-\omega)^2 r^2 \sin^2\theta e^{2(\beta-\nu)}}$$

↑

Differential rotation:
Mass varying from
1.4-2.6 $M_\odot$ for
0.004< ME/GE < 0.14

$P = k\rho^\Gamma$, $\Gamma \approx 4/3$, $^v{}_m \geq 20$

$B_{max} \sim 3\times10^{14}$ G, $B_s \geq 10^9$ G

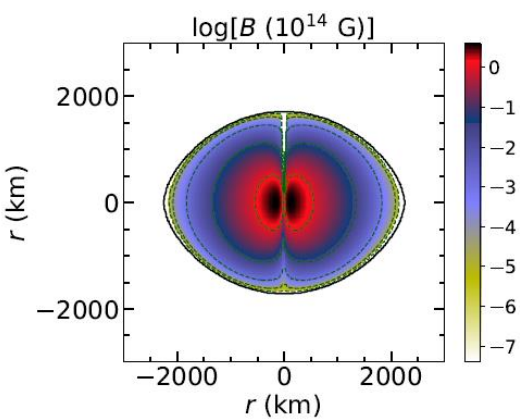

Polar hollow

M ≈ 2.5 $M_\odot$

$\rho_0 = 10^{10}$ gm/cc

Simulated by *XNS* code

Subramanian, BM, MNRAS 2015
Kalita, BM, MNRAS 2019

Nonrotating B-WDs in finite temperature

Magnetostatic balance
and photon diffusion equations:

$$\frac{\mathrm{d}}{\mathrm{d}r}(P_{\mathrm{deg}} + P_{\mathrm{ig}} + P_B) = -\frac{Gm(r)}{r^2}(\rho + \rho_B),$$

$$\frac{\mathrm{d}T}{\mathrm{d}r} = -\max\left[\frac{3}{4ac}\frac{\kappa(\rho+\rho_B)}{T^3}\frac{L_r}{4\pi r^2}, \left(1-\frac{1}{\gamma}\right)\frac{T}{P}\frac{\mathrm{d}P}{\mathrm{d}r}\right],$$

$$\frac{\mathrm{d}m}{\mathrm{d}r} = 4\pi r^2(\rho + \rho_B),$$

Boundary conditions:
ρ, R, M at surface for a given *L*

$$B\left(\frac{\rho}{\rho_0}\right) = B_{\mathrm{s}} + B_0\left[1 - \exp\left(-\eta\left(\frac{\rho}{\rho_0}\right)^{\gamma}\right)\right]$$

$B \equiv (B_s, B_0)$

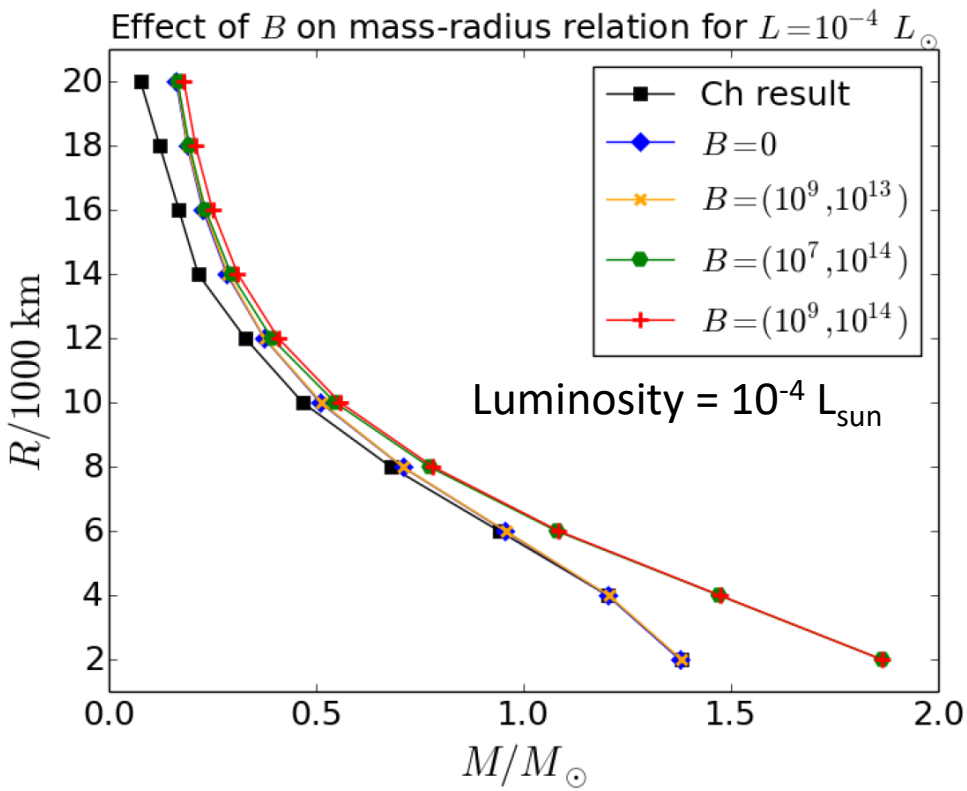

Theory and simulation by Cambridge STARS perfectly match

Eventually mass and corresponding central density to be restricted by, e.g. pycnonuclear reaction-based instability.

Gupta, BM, Tout, MNRAS 2020
Bhattacharya et al., MNRAS (submitted)

From conservation of total energy: presence of magnetic effect at the expense of thermal effect

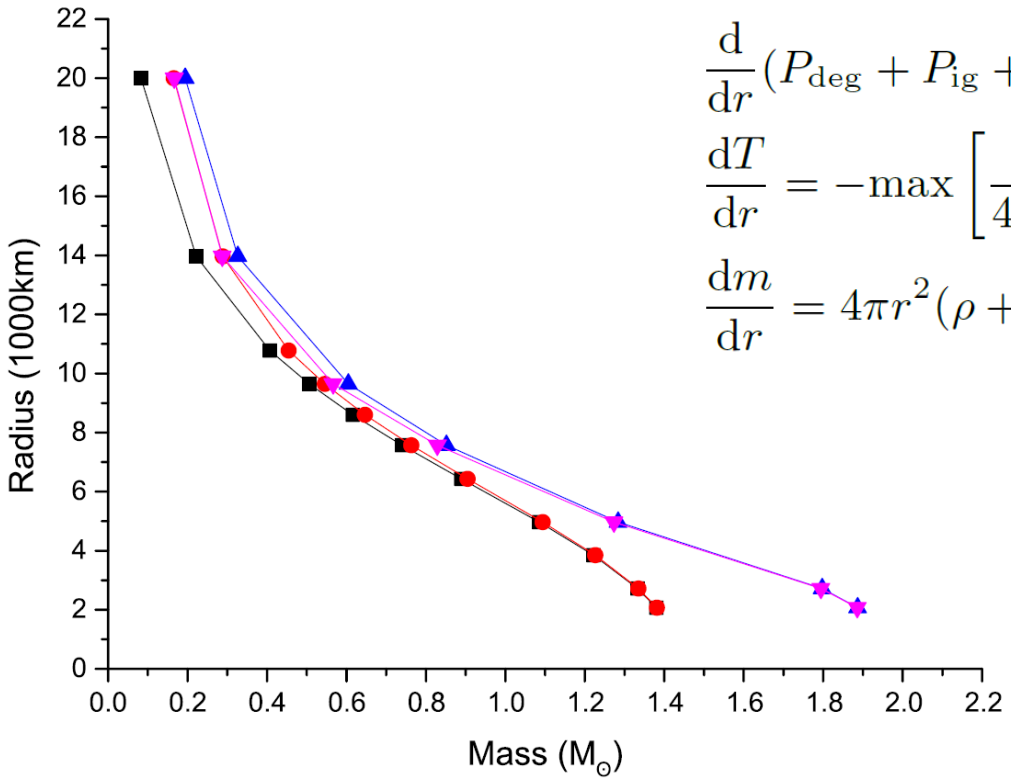

$$\frac{\mathrm{d}}{\mathrm{d}r}(P_{\rm deg} + P_{\rm ig} + P_B) = -\frac{Gm(r)}{r^2}(\rho + \rho_B),$$

$$\frac{\mathrm{d}T}{\mathrm{d}r} = -\max\left[\frac{3}{4ac}\frac{\kappa(\rho+\rho_B)}{T^3}\frac{L_r}{4\pi r^2}, \left(1-\frac{1}{\gamma}\right)\frac{T}{P}\frac{\mathrm{d}P}{\mathrm{d}r}\right],$$

$$\frac{\mathrm{d}m}{\mathrm{d}r} = 4\pi r^2(\rho + \rho_B),$$

Figure 5. The effect of magnetic field optimizing luminosity to attempt to match with Chandrasekhar's mass–radius relation (black squares), for $(B_s,\ B_0) = (10^9,\ 10^{14})$ G (magenta downward triangles), while the lines with red circles and blue upward triangles represent the results with $L = 10^{-4}\,L_\odot$ for $(B_s,\ B_0) = (0,\ 0)$ and $(10^9,\ 10^{14})$ G respectively. All cases correspond to $\mathrm{d}T/\mathrm{d}r = 0$ below the interface radius. See Table 3 for specific luminosities.

Gupta, BM, Tout, MNRAS 2020

From conservation of total energy: presence of magnetic effect at the expense of thermal effect

$R/1000\,\mathrm{km}$	$(B_s, B_0)/\mathrm{G}$	$L/L_\odot$	$M/M_\odot$	$M_{\mathrm{original}}/M_\odot$	$\rho_c/10^6\,\mathrm{g\,cm^{-3}}$	$\rho_c^{\mathrm{original}}/10^6\,\mathrm{g\,cm^{-}}$
20	$(10^9, 10^{14})$	8×10^{-6}	0.166	0.165	0.106	0.0983
20	$(10^7, 10^{14})$	7×10^{-5}	0.166	0.165	0.095	0.0983
13.965	$(10^9, 10^{14})$	10^{-6}	0.287	0.288	0.3934	0.4095
13.965	$(10^7, 10^{14})$	3×10^{-5}	0.289	0.288	0.3854	0.4095
9.645	$(10^9, 10^{14})$	10^{-12}	0.566	0.545	2.29	2.36
9.645	$(10^7, 10^{14})$	10^{-12}	0.551	0.545	2.121	2.36
7.57	$(10^9, 10^{14})$	10^{-12}	0.829	0.763	7.873	7.738
7.57	$(10^7, 10^{14})$	10^{-12}	0.818	0.763	7.7563	7.738
4.968	$(10^9, 10^{14})$	10^{-16}	1.273	1.094	57.19	55.35
4.968	$(10^7, 10^{14})$	10^{-12}	1.270	1.094	56.35	55.35
2.7215	$(10^9, 10^{14})$	10^{-16}	1.794	1.335	720.89	686.96
2.7215	$(10^7, 10^{14})$	10^{-12}	1.793	1.335	718.62	686.96
2.068	$(10^9, 10^{14})$	10^{-16}	1.886	1.381	2473.8	1962
2.068	$(10^7, 10^{14})$	10^{-16}	1.886	1.381	2462.4	1962

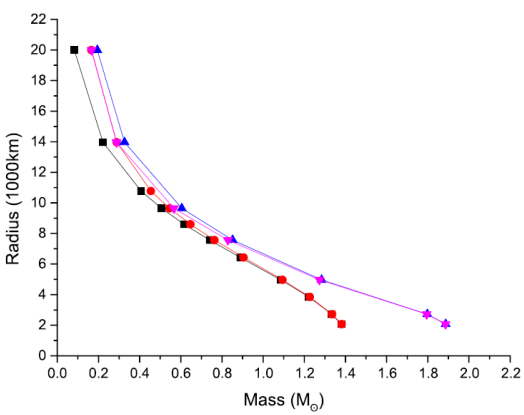

Very low luminosity: dim

Gupta, BM, Tout, MNRAS, 2020

Obtaining new limit: spirit of Chandrasekhar Quantum (EoS) effect: Constant or fluctuating fields

$$\frac{1}{\rho}\frac{d}{dr}\left(P+\frac{B^2}{8\pi}\right)=F_g+\frac{\vec{B}\cdot\nabla\vec{B}}{4\pi\rho},$$

$$\frac{dM}{dr}=4\pi r^2\rho$$

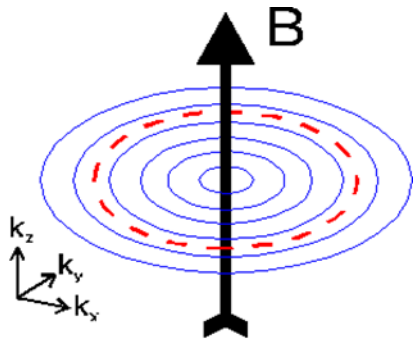

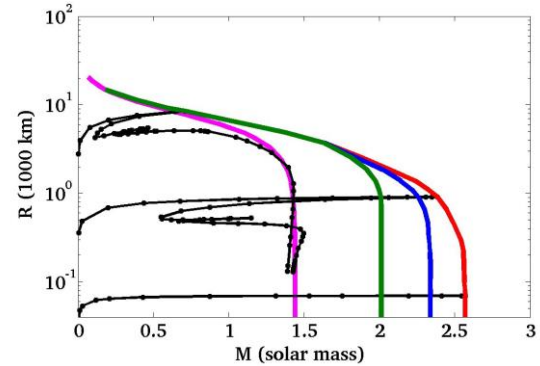

$$M\propto K^{3/2}\rho_c^{\frac{3-n}{2n}},\qquad R\propto K^{1/2}\rho_c^{\frac{1-n}{2n}}$$

$P = K\rho^{\Gamma}$

For extremely high density regime

$$K=K_m\propto B_D^{-1}\propto\rho_c^{-2/3}$$

At constant and fluctuating fields

Mass is independent of ρ_c and radius becomes zero

Ours

Γ=2 and hence n=1

$$M=\left(\frac{hc}{2G}\right)^{3/2}\frac{1}{(\mu_e m_H)^2}\approx\frac{10.312}{\mu_e^2}M_\odot,$$

Chandrasekhar's

Γ=4/3 and hence n=3

$$M_{\rm Ch}=\frac{\sqrt{6}}{32\pi}\left(\frac{hc}{G}\right)^{3/2}\left(\frac{2}{\mu_e}\right)^2\frac{\xi_1^2|\theta'(\xi_1)|}{m_{\rm H}^2}$$

For μ_e=2 (carbon-oxygen white dwarf)

$$M\approx 2.58M_\odot.$$

$$1.44M_\odot$$

Das, BM, PRL 2013

Effects of cooling and Ohmic and Hall decay

$$L = -\frac{d}{dt}\int c_{\rm v}\, dT = (2\times 10^6\ {\rm erg/s})\,\frac{A m_\mu}{M_\odot}\left(\frac{T}{K}\right)^{7/2}$$

$$(T/{\rm K})^{-5/2} - (T_0/{\rm K})^{-5/2} = 2.406\times 10^{-34}\,\tau/{\rm s}$$

$$\frac{{\rm d}B}{{\rm d}t} = -B\left(\frac{1}{t_{\rm Ohm}} + \frac{1}{t_{\rm Amb}} + \frac{1}{t_{\rm Hall}}\right)$$

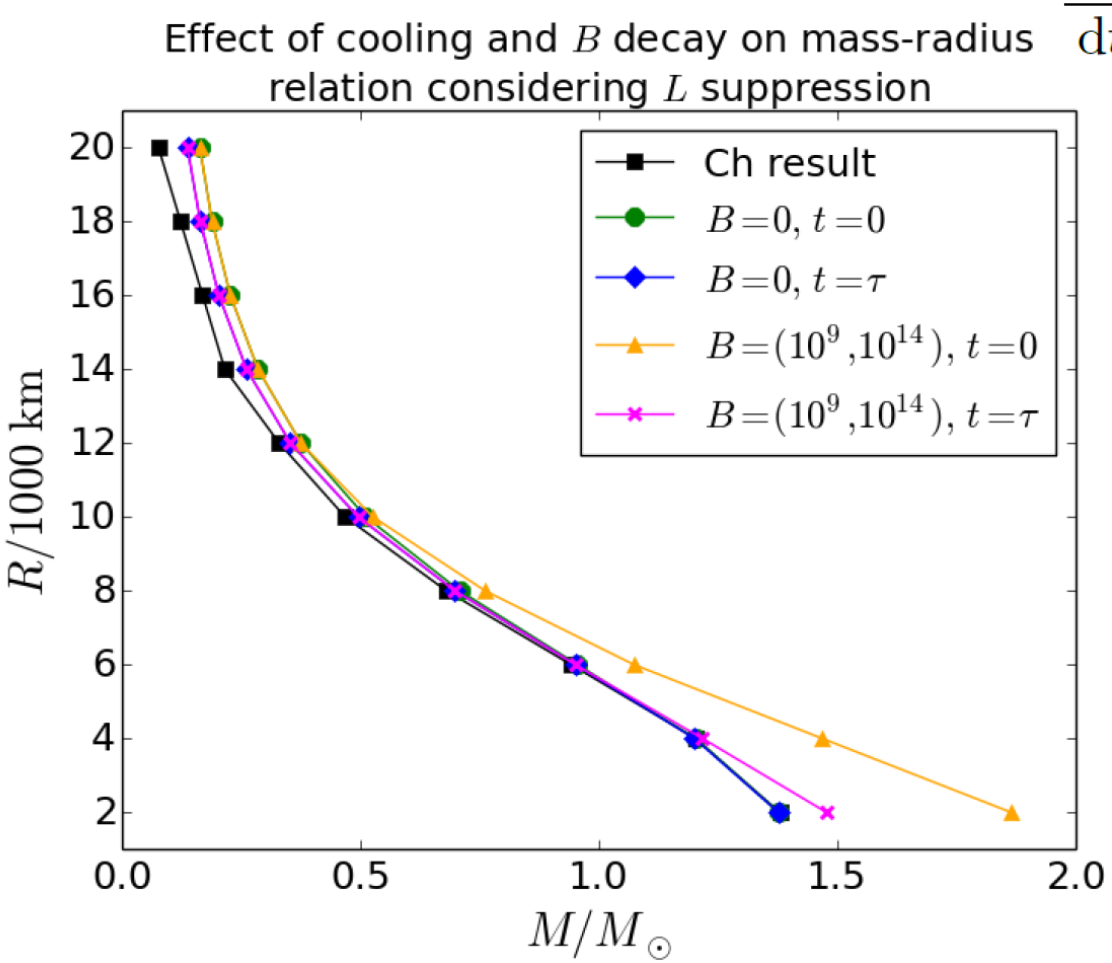

$$t_{\rm Ohm} = (7\times 10^{10}\ {\rm yr})\,\rho_{c,6}^{1/3} R_4^{1/2} (\rho_{\rm avg}/\rho_{\rm c})$$

$$t_{\rm Hall} = (5\times 10^{10}\ {\rm yr})\ l_8^2 B_{0,14}^{-1} T_{c,7}^2 \rho_{c,10}$$

Typically upto $10^{5\text{-}6}$ Year the mass remains unchanged → Beyond They are not massive

Bhattacharya et al., MNRAS (submitted)

Table 3. The effects of magnetic fields on the B-WD luminosity in order for the magnetised mass–radius relation to match with the non-magnetised relation. The initial field at $t = 0$ is kept fixed at $B = (10^9, 10^{14})$ G for all the radii listed here. The topmost entry for each radius is for the initial time $t = 0$ whereas the bottom two entries list the corresponding parameters for $t = \tau = 10$ Gyr after including the cooling rate and magnetic field decay over time. While we evaluate the magnetic fields assuming that Ohmic dissipation is the dominant process for the top entries of $\tau = 10$ Gyr, for the bottom entries, we assume that Hall drift is the primary process for the central field decay to $B_0 \gtrsim 10^{12}$ G below which Ohmic dissipation dominates.

$R/1000$ km	t/Gyr	$t_{\rm HO}/\tau$	$B_{\rm s}$/G	B_0/G	$L/L_\odot$	$M_{B=0}/M_\odot$	$M/M_\odot$
2.0	0		10^9	10^{14}	10^{-16}	1.378	1.865
	10	0	4.58×10^8	4.58×10^{13}	10^{-16}	1.377	1.478
		1		5.83×10^{13}	10^{-16}		1.542
4.0	0		10^9	10^{14}	10^{-16}	1.204	1.469
	10	0	2.78×10^8	2.78×10^{13}	10^{-12}	1.201	1.218
		0.224		3.71×10^{11}	3×10^{-7}		1.201
6.0	0		10^9	10^{14}	10^{-16}	0.956	1.074
	10	0	1.65×10^8	1.65×10^{13}	10^{-8}	0.951	0.951
		6.89×10^{-2}		1.86×10^{11}	2×10^{-6}		0.951
8.0	0		10^9	10^{14}	10^{-12}	0.709	0.762
	10	0	9.86×10^7	9.86×10^{12}	2×10^{-6}	0.699	0.699
		2.28×10^{-2}		1.04×10^{11}	7×10^{-6}		0.699
10.0	0		10^9	10^{14}	10^{-12}	0.512	0.527
	10	0	6.02×10^7	6.02×10^{12}	8×10^{-6}	0.496	0.496
		9.72×10^{-3}		6.18×10^{10}	10^{-5}		0.496
12.0	0		10^9	10^{14}	7×10^{-8}	0.376	0.376
	10	0	3.69×10^7	3.69×10^{12}	10^{-5}	0.354	0.354
		4.88×10^{-3}		3.75×10^{10}	10^{-5}		0.354
14.0	0		10^9	10^{14}	2×10^{-6}	0.286	0.286
	10	0	3.06×10^7	3.06×10^{12}	10^{-5}	0.262	0.262
		2.22×10^{-3}		3.08×10^{10}	10^{-5}		0.262
16.0	0		10^9	10^{14}	4×10^{-6}	0.228	0.228
	10	0	2.00×10^7	2.00×10^{12}	10^{-5}	0.204	0.204
		1.34×10^{-3}		2.01×10^{10}	10^{-5}		0.204
18.0	0		10^9	10^{14}	5×10^{-6}	0.190	0.190
	10	0	1.87×10^7	1.87×10^{12}	10^{-5}	0.165	0.165
		7.75×10^{-4}		1.88×10^{10}	10^{-5}		0.165
20.0	0		10^9	10^{14}	7×10^{-6}	0.164	0.164
	10	0	2.97×10^7	2.97×10^{12}	10^{-5}	0.138	0.138
		3.70×10^{-4}		2.98×10^{10}	10^{-5}		0.138

$$t_{\rm Ohm} = (7 \times 10^{10}\ {\rm yr})\, \rho_{\rm c,6}^{1/3} R_4^{1/2} (\rho_{\rm avg}/\rho_{\rm c})$$

$$t_{\rm Hall} = (5 \times 10^{10}\ {\rm yr})\, l_8^2 B_{0,14}^{-1} T_{\rm c,7}^2 \rho_{\rm c,10}$$

Continuous Gravitational Wave from B-WDs

Signal emitted by a tri-axial compact star rotating around a principle axis of inertia is characterized by the amplitude

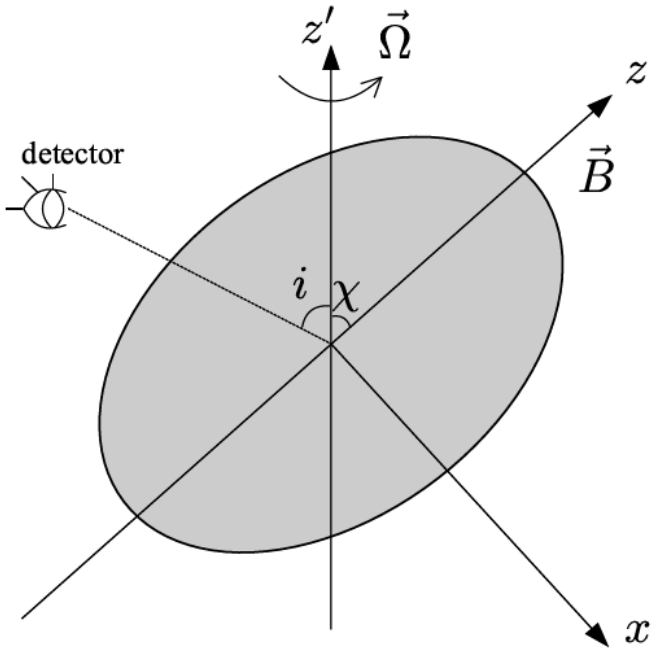

$$h_+ = h_0 \sin\chi \left[\frac{1}{2} \cos i \sin i \cos\chi \cos\Omega t - \frac{1+\cos^2 i}{2} \sin\chi \cos 2\Omega t \right],$$

$$h_\times = h_0 \sin\chi \left[\frac{1}{2} \sin i \cos\chi \sin\Omega t - \cos i \sin\chi \sin 2\Omega t \right], \quad (1)$$

with

$$h_0 = -\frac{6G}{c^4} Q_{z'z'} \frac{\Omega^2}{d}, \quad (2)$$

$$h_0 = \frac{2G}{c^4} \frac{\Omega^2 \varepsilon I_{xx}}{d} (2\cos^2\chi - \sin^2\chi),$$

For $\chi \rightarrow 0$

$$h_0 \rightarrow \frac{4G}{c^4} \frac{\Omega^2 \varepsilon I_{xx}}{d},$$

Consider small χ approximation cases

Small χ assures applicability of results from *XNS/LORENE* codes

BM, Rao, Bhatia, MNRAS 2017
Kalita, BM, MNRAS 2019
Kalita et al., ApJ, 2020; MNRAS 2021

Toroidally (centrally) dominated B-WDs with poloidal surface fields:

B_{cent} (Tor) ≥ 10^{14} G, B_{cent} (Pol) ~ 10^{12} G, B_{surf} (Pol) ≤ 10^{10} G

Table 5. WDs possessing toroidal magnetic field for $\rho_c = 2 \times 10^{10}$ g cm^{-3}. Here $B_{\max}$ is the strength of the maximum magnetic field in the WD and R_E is the equatorial radius. t_{vl} means the timescale is very large.

M ($M_\odot$)	R_E (km)	$B_{\max}$ (G)	P (s)	ME/GE	KE/GE	L_{GW} (erg/s)	h_0	t_{10} (year)
1.71	2095.4	2.6×10^{14}	2.0	1.0×10^{-1}	5.4×10^{-3}	3.1×10^{39}	1.7×10^{-20}	t_{vl}
1.44	1315.7	1.1×10^{14}	2.0	1.0×10^{-2}	2.7×10^{-3}	2.6×10^{35}	4.6×10^{-22}	t_{vl}
1.67	1767.6	2.6×10^{14}	10.0	1.0×10^{-1}	2.0×10^{-4}	2.3×10^{36}	7.5×10^{-22}	t_{vl}
1.43	1253.7	1.1×10^{14}	10.0	1.0×10^{-2}	1.0×10^{-4}	6.3×10^{32}	3.7×10^{-23}	t_{vl}

d=100pc

$10^{-5} < |I_{x'x'} - I_{y'y'}|/I_{z'z'} < 10^{-4}$

***L_D* and *L_{GW}* exhibited in quite different ranges**

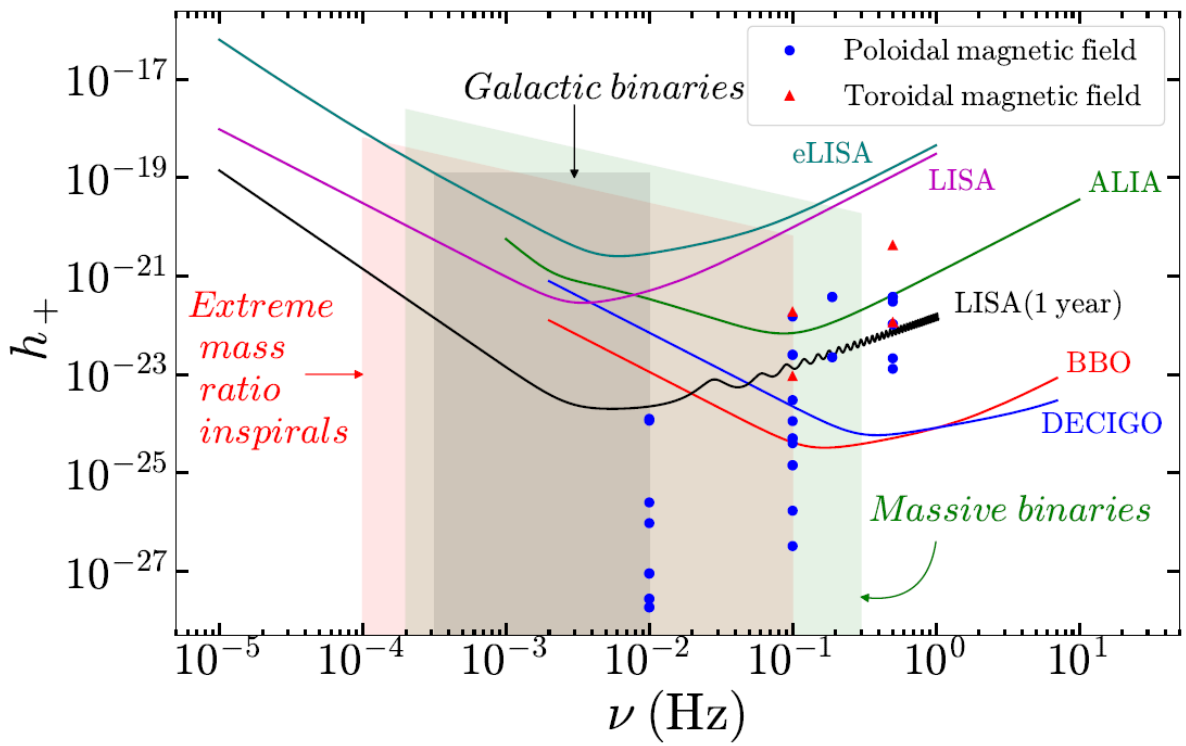

Kalita, BM, MNRS 2019
Kalita et al., ApJ, 2020

Wickramasinghe, Tout, Ferrario, MNRAS 2014

Powers of magnetized rotating white dwarfs

Behaving/Modelled like rotating dipole:

$$L_{\rm D} = \frac{B_p^2 R_p^6 \Omega^4}{2c^3} \sin^2\chi \; F(x_0), \;\; F(x_0) = \frac{x_0^4}{5\left(x_0^6 - 3x_0^4 + 36\right)} + \frac{1}{3\left(x_0^2+1\right)}$$

$$L_{\rm GW} = \frac{2G}{5c^5}(I_{zz} - I_{xx})^2 \Omega^6 \sin^2\chi \left(1 + 15\sin^2\chi\right)$$

$$\frac{d(\Omega I_{z'z'})}{dt} = -\frac{2G}{5c^5}\left(I_{zz} - I_{xx}\right)^2 \Omega^5 \sin^2\chi \left(1 + 15\sin^2\chi\right) - \frac{B_p^2 R_p^6 \Omega^3}{2c^3} \sin^2\chi \; F(x_0), \tag{6}$$

$$I_{z'z'}\frac{d\chi}{dt} = -\frac{12G}{5c^5}\left(I_{zz} - I_{xx}\right)^2 \Omega^4 \sin^3\chi \cos\chi - \frac{B_p^2 R_p^6 \Omega^2}{2c^3} \sin\chi\cos\chi \; F(x_0), \tag{7}$$

Melatos 2000

Zimmermann & Szedenits 1979

Kalita et al., ApJ, 2021

GW S/N for various compact objects

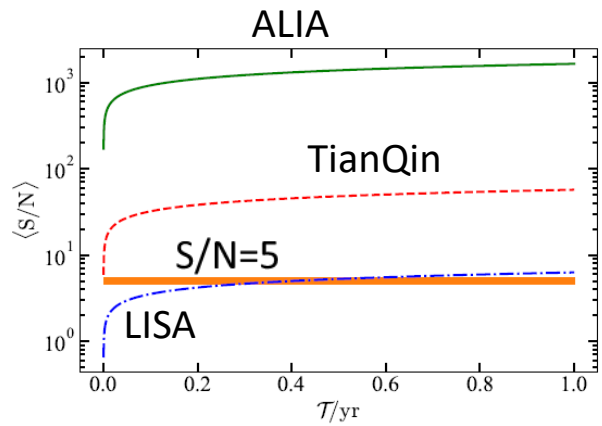

(a) $B_{max} = 2.6 \times 10^{14}$ G

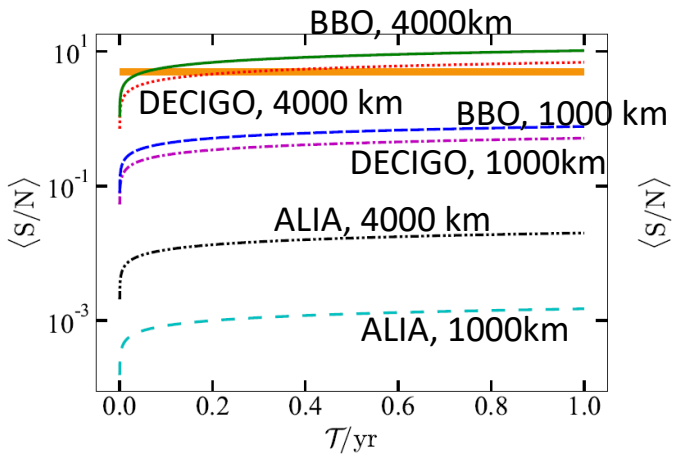

(a) Poloidal field dominated WD

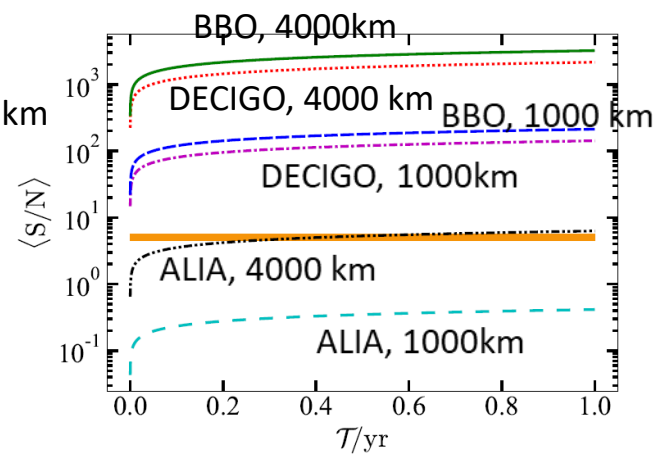

(b) Toroidal field dominated WD

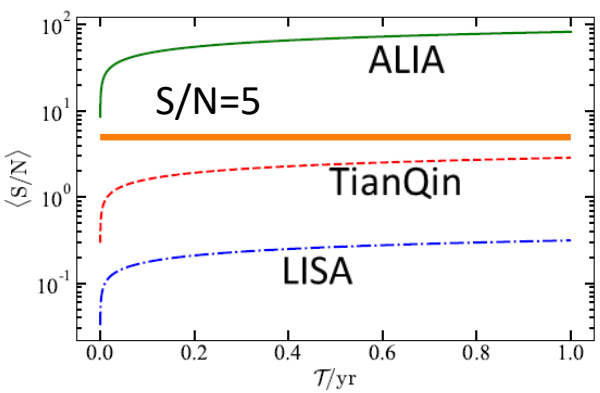

(b) $B_{max} = 1.1 \times 10^{14}$ G

XTE J1810 – 197

χ = 45, P = 5.54 s, d = 3.5 kpc

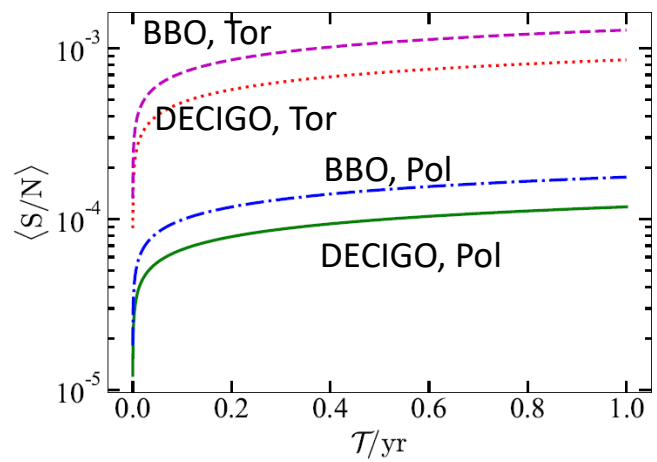

(c) NS with radius 14 km

P=2 s, χ = 30, d = 100 pc

Super-Chandrasekhar candidate

Kalita et al., ApJ, 2021

White dwarf with anisotropic effects

$$\frac{\mathrm{d}m}{\mathrm{d}r} = 4\pi\left(\rho + \frac{B^2}{8\pi}\right) r^2,$$

$$p_r = \frac{\pi m_e^4 c^5}{3h^3}\left[x\left(2x^2-3\right)\sqrt{x^2+1} + 3\sinh^{-1}x\right],$$

$$\rho = \frac{8\pi\mu_e m_H \left(m_e c\right)^3}{3h^3} x^3,$$

$$\begin{cases} \dfrac{\mathrm{d}p_r}{\mathrm{d}r} = \dfrac{-(\rho+p_r)\dfrac{4\pi r^3\left(p_r - \frac{B^2}{8\pi}\right)+m}{r(r-2m)} + \frac{2}{r}\Delta}{\left[1-\frac{\mathrm{d}}{\mathrm{d}\rho}\left(\frac{B^2}{8\pi}\right)\frac{\mathrm{d}\rho}{\mathrm{d}p_r}\right]}, & \text{for RO,} \\[2ex] \dfrac{\mathrm{d}p_r}{\mathrm{d}r} = \dfrac{-\left(\rho+p_r+\frac{B^2}{4\pi}\right)\dfrac{4\pi r^3\left(p_r + \frac{B^2}{8\pi}\right)+m}{r(r-2m)} + \frac{2}{r}\Delta}{\left[1+\frac{\mathrm{d}}{\mathrm{d}\rho}\left(\frac{B^2}{8\pi}\right)\frac{\mathrm{d}\rho}{\mathrm{d}p_r}\right]}, & \text{for TO.} \end{cases}$$

$\Delta = p_t - p_r - B^2/8\pi$ for TO

$\Delta = p_t - p_r + B^2/8\pi$ for RO

$$\Delta = \begin{cases} \kappa\dfrac{(\rho+p_r)\left(\rho+3\,p_r-\frac{B^2}{4\pi}\right)}{\left(1-\frac{2m}{r}\right)} r^2, & \text{for RO,} \\[2ex] \kappa\dfrac{\left(\rho+p_r+\frac{B^2}{4\pi}\right)\left(\rho+3\,p_r+\frac{B^2}{2\pi}\right)}{\left(1-\frac{2m}{r}\right)} r^2, & \text{for TO,} \end{cases}$$

Deb, BM, Weber, ApJ, 2021

White dwarf with anisotropic effects

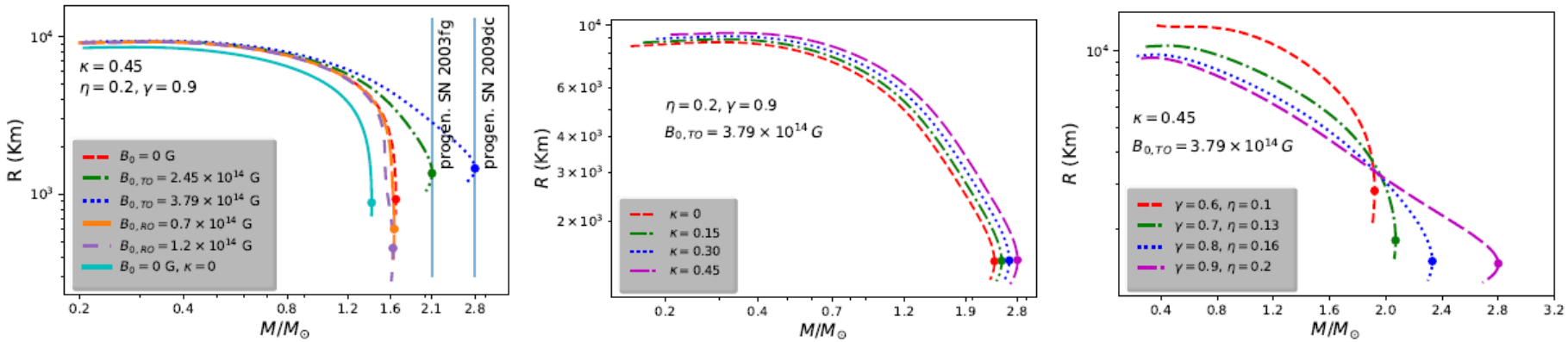

Figure 5. Variation of the total mass in the units of solar mass $(M/M_\odot)$ with the total radius (R) of the stars for (a) varying B_0 and $\kappa = 0.45$ (left panel), (b) varying κ and $B_0 = 3.79 \times 10^{14}\ G$ (middle panel) and (c) varying η and γ, where $B_0 = 3.79 \times 10^{14}\ G$ and $\kappa = 0.45$ (right panel). Solid circles represent maximum possible mass for the stars.

Deb, BM, Weber, ApJ (to be submitted)

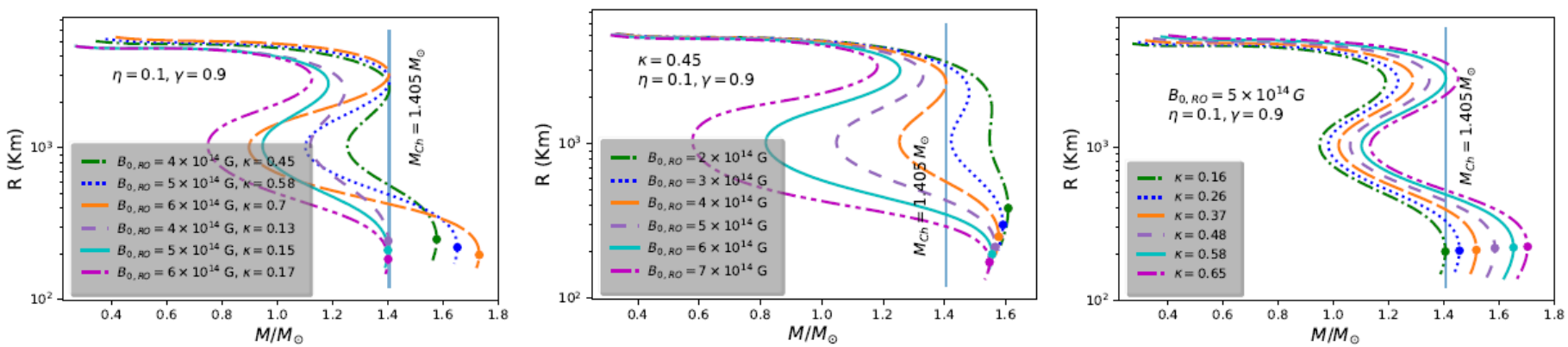

Figure 6. Variation of the total mass in the units of solar mass $(M/M_\odot)$ with the total radius (R) of the stars for (a) varying B_0 and κ (left panel), (b) varying B_0, where $\kappa = 0.45$ (middle panel) and (c) varying κ, where $B_0 = 5 \times 10^{14}\ G$ (right panel). Solid circles represent maximum possible mass for the stars.

Summary and Conclusions

- Highly magnetized, stable white dwarfs (B-WDs) and neutron stars have a variety of implications, including enigmatic peculiar over-luminous SNeIa
- Numerical simulation of Cambridge STARS argue B-WDs to be toroidally (centrally) dominated with lower surface (maybe dipole) fields
- New, generic, mass limit of white dwarfs seems to be more than $2M_{\odot}$
- They are triaxial, determined by their stable equilibria conditions
- They are difficult to observe or rare, due to decaying fields, hence not remained massive longer, and/or fast losing pulsar nature, and/or low luminosity
- They could be very good candidates for LISA (1 year integration), but also for Einstein Telescope and future DECIGO/BBO missions
- Hence, appropriate mission in GW astronomy and otherwise, e.g. radio astronomy, should be planned to probe them

Representative References

1. U. Das, BM, PRD, 042001, 2012
2. U. Das, BM, PRL, 071102, 2013
3. U. Das, BM, JCAP, 06, 050, 2014
4. S. Subramanian, BM, MNRAS, 454, 752, 2015
5. BM, A. R. Rao, JCAP, 05, 007, 2016
6. BM, A. R. Rao, T. S. Bhatia, MNRAS, 472, 3564, 2017
7. M. Bhattacharya, BM, S. Mukerjee, MNRAS, 477, 2705, 2018
8. S. Kalita, BM, MNRAS, 490, 2692, 2019
9. A. Gupta, BM, C. A. Tout, MNRAS, 496, 4191, 2020
10. BM, A. Sarkar, C. A. Tout, MNRAS, 500, 763, 2021
11. Deb, BM, Weber, ApJ (accepted for publication), 2021